Sub-barrier fusion in a macroscopic model of nuclear shape evolutions

V. S. Ramamurthy,* A. K. Mohanty, S. K. Kataria, and G. Rangarajan†
Nuclear Physics Division, Bhabha Atomic Research Centre, Trombay, Bombay 400085, India
(Received 9 January 1990)

The macroscopic model of nuclear shape evolutions describing nuclear coalescence and reseparation in heavy-ion collisions is applied to the sub-barrier region. The model brings out the important role of neck formation on sub-barrier fusion in addition to effects arising from collective excitations of the colliding partners and nucleons transfer in the entrance channel.

I. INTRODUCTION

It is now well known that,[1,2] while the large body of experimental fusion excitation functions of nuclear collisions at bombarding energies close to the Coulomb barrier can be systematized in terms of a one-dimensional energy-independent fusion barrier, the fusion cross sections measured at sub-barrier energies decrease much less steeply than what is expected on the basis of a quantum-mechanical penetration of the same one-dimensional fusion barrier. An analysis of the available data has also shown that the "anomalous" sub-barrier fusion enhancement is a general phenomenon, exhibiting a rather complex dependence on the nuclear species of the projectile and the target, both a global dependence following a monotonic pattern with increasing mass and charge of the reacting partners and a local dependence explicitly involving their structural details. The problem is one of enumerating the factors which affect fusion and working out theoretical models to make quantitative predictions.

In studying the fusion excitation functions of a number of systems, the one-dimensional barrier penetration model is acceptably adequate provided one is allowed some freedom in the choice of the interaction potential parameters. An indication that the underlying physics may be more complex comes from the fact that it is rather difficult to find a global potential that describes all the systems. In fact, for several systems, attempts[3] to reconstruct the potential by inverting the experimental cross sections have resulted in fusion barriers which are unrealistically thin, sometimes even reentrant. A reentrant barrier clearly signals the availability of additional degrees of freedom to the system, over and above the relative separation during the fusion process. Candidates which provide additional degrees of freedom to the colliding nuclei are nuclear deformations,[4] quantal zero-point shape oscillations,[5,6] and nucleon transfer. The coupled-channel approach[7] to direct reactions offers a formal theoretical basis for studying the effect of these collective modes on fusion. An important deficiency of the coupled-channel approach to the sub-barrier fusion problem is the way in which the fusion channel is treated in these calculations. Like the simple one-dimensional barrier penetration model, the coupled-channel approach, as used up to now, is also a barrier passing theory; that is, the barrier acts as a divider of the total reaction cross section into two groups: (i) the direct, quasielastic reactions and (ii) fusion. Flux penetrating inside the barrier is assumed to lead to fusion and is prevented from being reflected by either an ingoing wave boundary condition or a short-ranged imaginary potential operating at radii well inside the barrier. Some authors also allow for fusion under the barrier by adjusting the imaginary potential to fit experimental fusion excitation functions. This approach obviously shields all the dynamical details of the fusion process beyond the passage over the fusion barrier. In this work, we have applied macroscopic model of nuclear shape evolutions to the sub-barrier fusion problem with the inclusion of tunneling. The explicit inclusion of the neck degree of freedom in the model results in alternative paths for fusion and therefore energy-dependent fusion barrier. The model brings out the important role of neck formation on sub-barrier fusion in addition to effects arising from collective excitations of the colliding partners and nucleon transfer in the entrance channel.

II. FUSION IN A DYNAMICAL MODEL OF SHAPE EVOLUTIONS

A macroscopic model of nuclear shape evolutions has been developed by Swiatecki[8] to describe the heavy-ion fusion process. The model not only brought out, in a simple and systematic way, the macroscopic features of most of the near barrier fusion excitation function data but also led to the prediction of the extra and the extra-extra push energies in heavy-ion collisions arising from dynamical limitations to the fusion process and to compound nucleus formation. Being classical, the implications of the model at sub-barrier energies were not investigated though it has been recognized for sometime[9-11] that the dynamics of neck formation may play a role in deciding the fusion cross sections even at sub-barrier energies. In the present work, it has been shown that, even at a qualitative level, the model leads to several interesting aspects of the sub-barrier fusion problem, provided one allows for the quantum-mechanical tunneling of a multidimensional potential barrier.

Swiatecki's shape parametrization consisting of two spheres connected by a conical neck, has the three degrees of freedom (see Fig. 1): (1) the relative separation variable $\rho = r/(R_1 + R_2)$, (2) the neck thickness variable $\alpha = \sin\theta/\sin\theta_{\max}$, and (3) the asymmetry variable

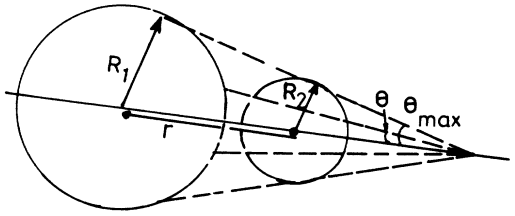

FIG. 1. Nuclear configurations represented by the three Swiatecki parameters.

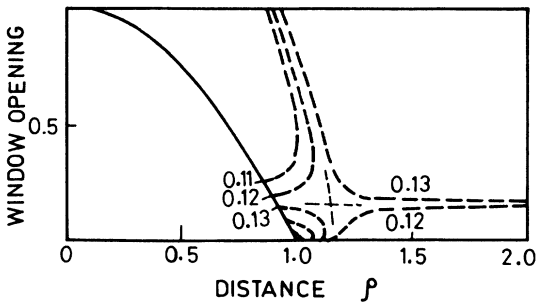

FIG. 2. Contour plot of the deformation potential energy in the two-dimensional space of relative separation and neck thickness for a typical symmetric system with $X=0.4$.

$\Delta=(R_1-R_2)/(R_1+R_2)$, where R_1 and R_2 are the radii of the two spheres. r is the center-to-center separation. θ is the semiopening angle of the conical neck and $\theta_{\max}=(R_1-R_2)/r$ refers to a fully open window. The variable Δ ranges from -1 to $+1$, α ranges from 0 to 1, and ρ from 0 to ∞. The parametrization smoothly connects the mononuclear regime and the dinuclear regime and can adequately describe the fusion of two nuclei. The macroscopic deformation potential energy as a function of the three shape parameters can be calculated as the sum of an electrostatic energy and a nuclear surface energy. Swiatecki has given, with the use of a new set of variables ν and σ and a third-order expansion of the potential energy in the neck size, the following expression for the potential energy (PE) taken with respect to the energy of tangent spheres $\mathrm{PE}_{\mathrm{tg}}$

$$\eta=\frac{\mathrm{PE}-\mathrm{PE}_{\mathrm{tg}}}{8\pi\bar{R}_\gamma^2}=\nu\sigma-\nu^2+\nu^3-X\sigma\ , \tag{1}$$

where

$$\nu=\alpha\ \ (0\le\nu\le1)\ ,$$

$$\sigma=\frac{\rho^2-1}{1-\Delta^2}\ \ (-1\le\sigma\le\infty)\ ,$$

$$\bar{R}=R_1R_2/(R_1+R_2)\ ,$$

and γ is the nuclear surface energy coefficient. The quantity X is the effective fissility parameter given by

$$X=\frac{Z_1Z_2e^2/(R_1+R_2)^2}{4\pi\gamma\bar{R}}\ ,$$

where Z_1 and Z_2 are the atomic numbers of the colliding nuclei. Figure 2 shows a contour plot of the calculated deformation potential-energy function for a typical medium mass nucleus. The potential-energy landscape exhibits two regions of low potential energy separated by a saddle-point pass—one corresponding to a fused composite system and the other corresponding to a configuration of separated fragments at infinity. Since, in general, the potential energy is not stationary with respect to the asymmetry degree of freedom, the saddle point is only a "conditional" saddle point, with the physical meaning of a mountain pass, only if the asymmetry is effectively held fixed.

Another interesting aspect of the potential landscape is the existence of two distinct valleys misaligned with respect to each other, the liquid-drop-model (LDM) fission valley of connected shapes and the two-fragment valley or the fusion valley of disconnected shapes separated by an energy ridge over narrow range of relative separation around $\sigma=0$. The contact configuration ($\sigma=0$, $\nu=0$) located on the two-fragment valley can be identified with the conventional one-dimensional fusion barrier. In a typical collision process, the system is injected along the fusion valley, climbing the one-dimensional fusion barrier. Since, in this valley, the two colliding nuclei are disconnected, there is no nuclear interaction between them in this model and the motion is nondissipative, with the kinetic energy in relative motion being continuously converted into potential energy. If the energy is sufficient to bring the system up to the contact configuration, the system becomes unstable with respect to the neck degree of freedom and the collision trajectory makes a sudden swerve towards the LDM fission valley. Motion in the LDM valley is highly damped. Trajectories which make contact and enter the LDM valley divide further into two more classes, depending on which side of the "conditional" saddle point the system enters the LDM valley. Those trajectories that pass over the conditional saddle point are captured, while those which do not reseparate as highly damped products accompanied also by appreciable nucleon exchange. For nearly symmetric systems, when the conditional saddle is essentially the unconditional saddle point, capture inside the conditional saddle point is synonymous with compound nucleus formation. However, for asymmetric systems, the conditional saddle point deviates from the true fission saddle. The captured trajectories then divide into two further classes: those that continue to be captured inside the fission saddle point and also lead to compound nucleus formation and those that are outside the fission saddle point and therefore reseparate into two fragments, fully relaxed in both relative kinetic energy and mass asymmetry (fissionlike fragments). Thus, a necessary condition for fusion in this model is that the system should pass over the conditional saddle point while the condition for compound nucleus formation is that it should also pass over the unconditional saddle point. The fact that, for some systems, the conditional and the unconditional saddle points could become more compact than the contact configuration leads to the so-called extra and extra-extra push energies for fusion and compound nucleus formation, respectively, in

the Swiatecki model. The fact that, for light systems, the contact configuration is more compact than the other two saddle points is responsible for the overall success of the one-dimensional fusion barrier models for these systems. Swiatecki's calculations also showed that the time scales involved for motion in the three degrees of freedom are distinctly different—partly because of the differences in the relevant inertial masses and partly because of the differences in the nature of the dissipative forces. In particular, the motion in the neck degree of freedom is the fastest and, consequently, the neck growth takes place almost at constant relative separation once it becomes unfrozen.

If the injection energy is not sufficient to bring the system up to the contact configuration, the system, in general, is reflected back along the fusion valley, and the collision results in a peripheral interaction. However, quantum-mechanical tunneling can still enable the system to reach the contact configuration, passing through the classically forbidden region and proceed into the LDM valley. The multidimensional potential energy landscape shown in Fig. 2 also points out that this is not the only path for the system to reach the LDM valley. The system can first develop, at the classical turning point, a neck, and tunnel through the ridge separating the fusion valley from the LDM valley. Once in the LDM valley, the system will automatically be driven towards more compact configurations by the potential gradient, provided the system enters the LDM valley at a configuration more compact than the conditional saddle point. Since the height of the ridge decreases with increasing separation and the effective mass for motion along the separation coordinate is much larger than that along the neck degree, the alternate path bypassing the contact configuration has a higher probability of tunneling than the path passing through the contact configuration. In fact, the system has several paths in two dimensions to pass from the two-fragment valley into the LDM valley, all of which are to be considered with their respective tunneling probabilities. For still lower bombarding energies, when the classical turning point becomes less compact than point C (see Fig. 3), it is necessary for the system to tunnel along the separation degree to enter the LDM valley. Thus, the bombarding energy domain separates into three distinct regions.

(a) Region I: Bombarding energy more than that required to bring the system up to the contact configuration.

(b) Region II: Bombarding energy less than that required to bring the system up to the contact configuration but sufficient to take it into the fission valley through the ridge at the classical turning point.

(c) Region III: Bombarding energy less than that required to take the system into the fission valley at the classical turning point.

In region I, fusion takes place classically. In regions II and III, fusion has to take place only by tunneling the potential-energy landscape. However, instead of penetrating through the one-dimensional "frozen density" potential barrier, the system now faces a potential surface; that is, a barrier ridge. An incoming wave packet probes at least part of this ridge and, in general, the transmission probability will be enhanced as compared to the one-dimensional frozen density result. For very low energies in Region III, the path crossing the ridge at its minimum possible value will dominate the excitation function. This minimum height of the ridge corresponds to the completely relaxed configuration, the adiabatic barrier. Thus, fusion enhancement arising mainly due to the additional neck degree of freedom which not only provides alternate paths with lower effective barriers but also has a smaller effective mass, is confined to a narrow region of bombarding energies in region II only. One can make a few general comments on the magnitude of the enhancement region II and its dependence on the target-projectile combination, based on the analytical expression for the potential energy [Eq. (1)]. Figure 3 shows a plot of the deformation energy versus relative separation along the fission and fusion valleys for a typical symmetric system with $X=0.54$. Figure 4 shows the effective barrier height versus the bombarding energy. The three regions I, II, and III are clearly seen in the figure. Figure 5 shows a plot of the width of the enhancement region versus the effective fissility X. It can be seen that the width of the enhancement region increases monotonically with increasing effective fissility X of the system. However, only for $X<0.5$, the enhanced capture into the fission

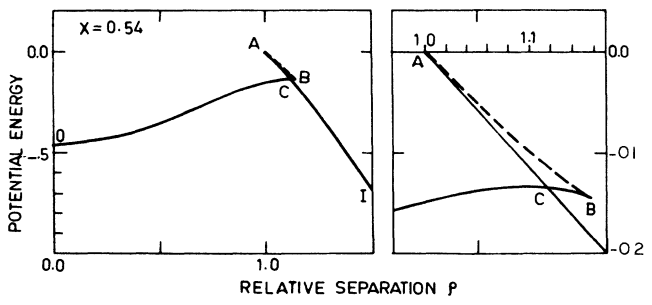

FIG. 3. Deformation potential energy versus relative separation along the fusion and the fission valleys for a typical symmetric system with $X=0.54$.

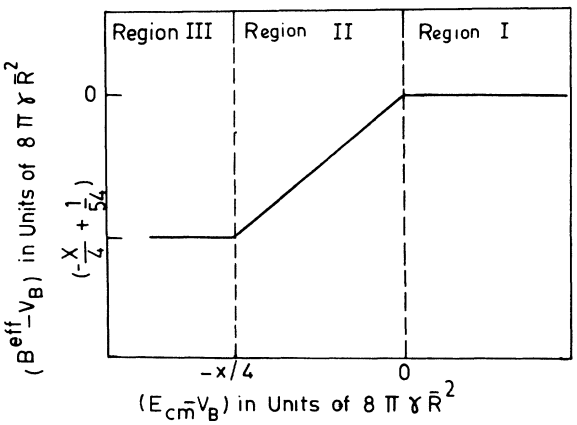

FIG. 4. Effective fusion barrier versus the center-of-mass bombarding energy.

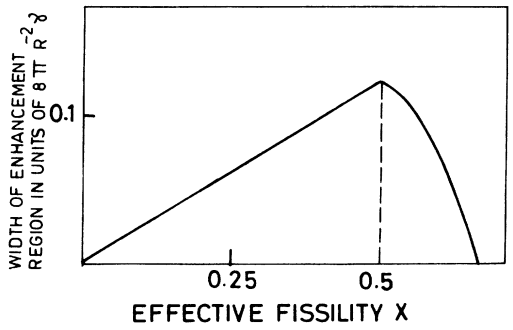

FIG. 5. Width of the fusion enhancement region versus the effective fissility of the system.

valley results in fusion. For $0.5<X<0.66$, part of the capture cross section results in deep-inelastic collision (DIC), since the conditional saddle point becomes more compact than point C. For $X>0.66$, tunneling through the ridge takes the system to the right of the conditional saddle point only and the entire enhancement in capture goes into DIC. Thus, while fusion enhancement is restricted to low and medium mass nuclear collisions, capture enhancement is a more general phenomenon occurring for all systems. Since these discussions are crucially dependent on the shape parametrization, we have also carried out deformation potential-energy calculations based on a more realistic shape parametrization, the *c-h* parametrization of Brack *et al.*,[12] where the nuclear surface is represented by a fourth-order polynomial given by

$$F^2(Z)=\lambda[Z_0^2-(Z+Z_s)^2][Z_2^2+(Z+Z_s-Z_1)^2] .$$

The normalization factor λ guarantees volume conservation and the variable Z_s is introduced to fix the center of mass at $Z=0$. The parameters Z_0, Z_2, and Z_1 are related to elongation, neck, and asymmetry degrees of freedom. The nuclear part of the potential energy includes the curvature energy terms also with a curvature tension of 10 MeV. The qualitative features of the PE landscape are the same as obtained earlier.

III. RESULT AND DISCUSSION

At this stage it is very tempting to carry out quantitative calculations of the sub-barrier fusion crosssections based on Swiatecki's model which will require calculation of the transmission coefficients in a two-dimensional potential barrier. But, as mentioned earlier, we will be missing all dynamical effects in the entrance channel arising from the structural details of the colliding partners; convincing evidence for which exists in the measured fusion cross sections. While the coupled-channel calculations given an adequate description of these and their influence on fusion, they ignore all dynamics after passage over the fusion barrier, the present model treats this aspect in more detail. A hybrid approach suggests itself but is yet to be developed. We therefore present here an analysis of the experimental data on fusion excitation functions which will demonstrate the role of neck formation in fusion dynamics without attempting an *ab initio* calculation of the same.

The discussions presented above demonstrate that, based on the bombarding energy, the system samples an energy-dependent effective barrier which coincides with the one-dimensional sudden potential barrier at bombarding energies near and above it while it coincides with the adiabatic potential barrier at bombarding energies very much below. At intermediate bombarding energies, a smooth transition of the effective barrier takes place from the sudden barrier to the adiabatic barrier as the bombarding energy is decreased. We have used the following method to go from the fusion excitation functions to the effective barriers, a procedure very similar to that of Balantekin *et al.* for one-dimensional barriers. We start with the following well-known expression for the fusion cross section

$$\sigma_F(E)=(\pi/k^2)\int dl(2l+1)T_l(E) . \quad (2)$$

Under the usual assumption that the different centrifugal barriers at a particular E have the same shape, one has

$$T_l(E)=T_0[E-l(l+1)\hbar^2/2\mu r^2] , \quad (3)$$

where r in the denominator can be replaced by a constant R at a particular energy $R^2(E)$. $R(E)$ is the region of the classical turning point at sub-barrier energies. One then obtains

$$\sigma_F(E)=[\pi R^2(E)/E]\int dE' T_0(E') . \quad (4)$$

Therefore,

$$\frac{d}{dE}\left|\frac{E\sigma}{\pi R^2(E)}\right|=T_0(E) . \quad (5)$$

Using the Hill-Wheeler form of penetration factor[13] for the case of a potential barrier with a quadratic maximum,

$$T_0(E)=\{1+\exp[2\pi(B_{\rm eff}-E)/\hbar\omega]\}^{-1} , \quad (6)$$

one obtains, for sub-barrier energies,

$$B_{\rm eff}=E+(\hbar\omega/2\pi)\ln\{[1-T_0(E)]/T_0(E)\} . \quad (7)$$

Thus, with R and $\hbar\omega$ specified, the effective barrier height $B_{\rm eff}$ is uniquely determined by the experimental data. In the present analysis, we have neglected the small energy dependence of the parameters R and $\hbar\omega$ and applied the method to determine the implied energy-dependent barriers for a number of systems, both light and heavy. For R, we use the fusion barrier radius R_B as deduced from above barrier fusion data and $\hbar\omega$ is determined from the extreme sub-barrier data. Figure 6 shows the deduced effective barriers for ^{40}Ar+^{144}Sm and ^{40}Ar+^{154}Sm. It is clearly seen from the figure, that the effective barriers show an energy dependence, consistent with the discussions presented above, namely, a constant value (adiabatic barrier) at low bombarding energies, the one-dimensional barrier at high bombarding energies, and a smooth transition in between. The effective decrease $\Delta B_{\rm eff}$ in barrier height (the difference between the one-dimensional barrier and the adiabatic barrier) calcu-

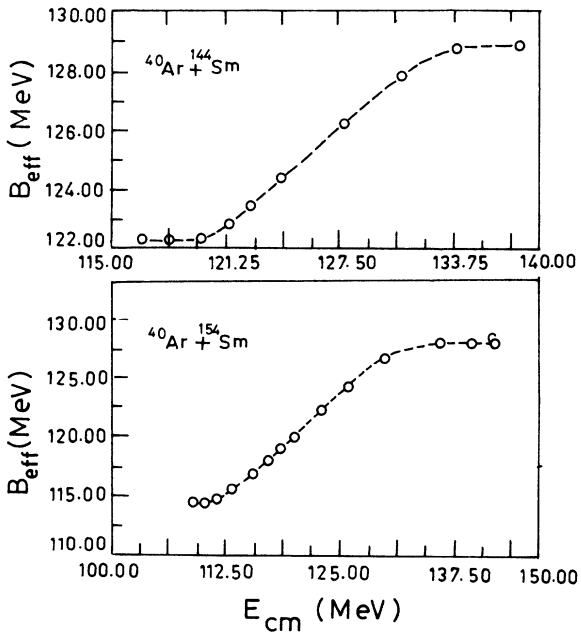

FIG. 6. "Experimental" effective fusion barriers versus the center-of-mass bombarding energy for two typical systems.

lated by the above procedure as a function of fissility parameter X has been plotted in Fig. 7. The solid line is the result on the basis of using Swiatecki's parametrization. The dashed line is with the *c-h* parametrization. While the calculated values of ΔB_{eff} are dependent on exact shape parametrization and the values of the LDM surface and curvature energy coefficients, the experimental values include the effects of entrance channel dynamics on

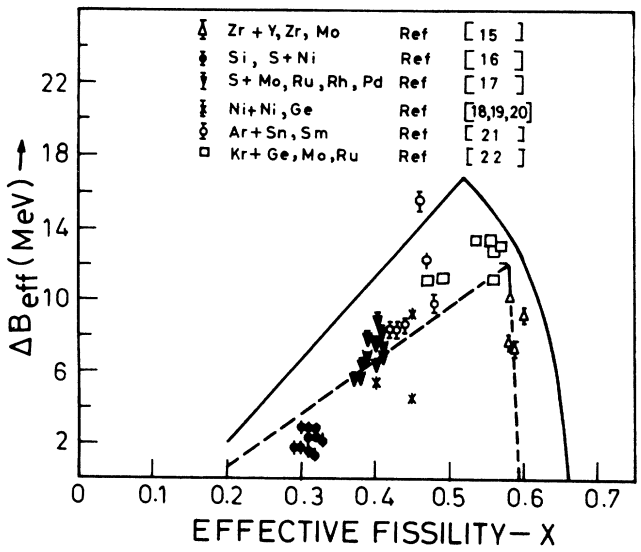

FIG. 7. Decrease in effective fissility X for different systems. The solid line is the result of using Swiatecki's parametrization. The dashed line is due to using parametrization given in Ref. 12 (See Refs. 15–22.)

fusion but the calculated values exhibit the same over all trend. The interesting feature in the above figure is that the enhancement increases as a function of fissility X up to a critical value of X, beyond which a rapidly decreasing fraction of the enhancement goes into the fusion channel. Again there is a second limit, beyond which there should be no enhancement in the fusion channel, all the enhancement going over to the DIC. In a similar investigation, Aguair *et al.*[14] have extracted the width of the enhancement region for a number of systems as a function of Bass fissility parameter. While the initial value of ΔB_{eff} vs X is in good agreement with our result, their analysis fails to bring out the fall beyond X_c. But as shown earlier, such a fall is expected from the model and is also supported by the limited available data. Experimental studies of sub-barrier DIC, however, have not received as much attention as sub-barrier fusion so far, but are likely to lead to interesting information on the dynamical aspects of nuclear collisions, in their early stages.

An energy-dependent effective barrier for fusion also has interesting sequences on fusion l distribution. Figure 8 shows a typical calculated l distribution. It can be seen that a finite width of the enhancement leads to an increased width of the l distribution; the increase being nearly proportional to the width. As has been shown, fusion enhancement and an increased width of the l distribution are caused by neck formation. It is also known

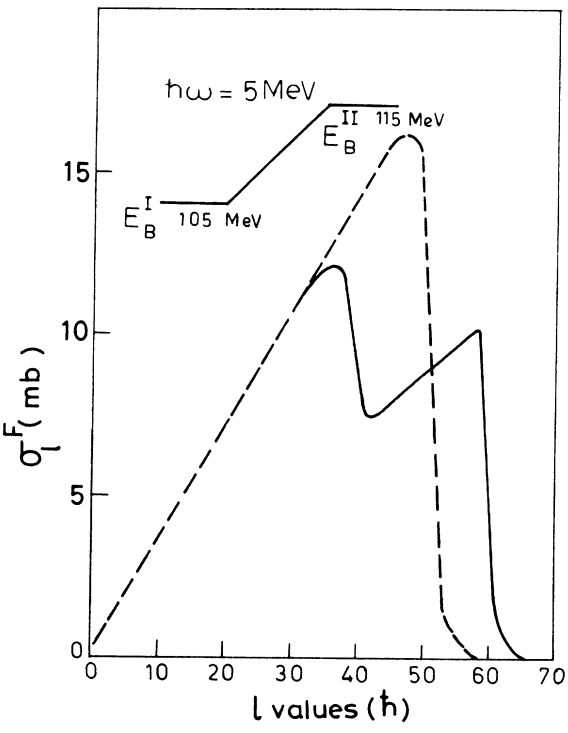

FIG. 8. The plot of σ_l vs l for a typical system at $E_{\text{c.m.}} = 125$ MeV using the parameters $V_B = 105$ MeV for $E_{\text{eff}} < 105$ MeV, $V_B = E_{\text{eff}}$ for 105 MeV $< E_{\text{eff}} < 115$ MeV, and $V_B = 115$ MeV for $E_{\text{eff}} > 115$ MeV. The dashed curve is obtained using an energy-independent barrier of $V_B = 110$ MeV.

that entrance channel dynamics leads to similar fusion enhancement and increased width of l distribution. An unambiguous signature of the effect of neck formation on fusion is the sudden drop in fusion enhancement as well as the $\langle l^2 \rangle$ for effective fissility $X_{\text{eff}} > 0.5$. It will be, therefore, very interesting to carry out discriminating experiments to measure fusion excitation functions and $\langle l^2 \rangle$ measurements for systems X_{eff} in the region of 0.5–0.6 which can provide direct proof of the role of neck degree of freedom on fusion.

IV. CONCLUSIONS

We have applied a macroscopic model of nuclear shape evolutions to describe fusion in heavy-ion collisions in the sub-barrier region. In this model the effective barrier for fusion at sub-barrier energies decreases due to neck formation, giving rise to broad spin distribution as well as enhanced fusion cross sections. We have also calculated the width of the enhancement region which increases as a function of X_{eff} up to a critical value which lies between 0.5 and 0.6, beyond which there is no enhancement. The model does not take into account the structural properties of the colliding partners and their influence on fusion. A work is in progress to develop a hybrid model to include structural effects via coupled-channels calculations and effects of neck formation through r-dependent imaginary potential for fusion.

We are thankful to Prof. M. A. Nagarajan and Dr. S. S. Kapoor and Sh. Suryanarayana for discussions during the course of these studies.

*Present address: Institute of Physics, Bhubaneswar, India 751005.

†Present address: Department of Physics and Astronomy, University of Maryland, College Park, MD 20742.

[1] L. C. Vaz and John M. Alexander, Phys. Rep. **69**, 373 (1981).

[2] *Fusion Cross Sections Below the Coulomb Barrier,* Vol. 219 of *Lecture Notes in Physics,* edited by S. G. Steadman (Springer-Verlag, Heidelberg, 1985).

[3] A. B. Balantekin, S. E. Koonin, and J. W. Negele, Phys. Rev. C **28**, 1565 (1983).

[4] C. Y. Wong, Phys. Rev. Lett. **31**, 766 (1973).

[5] H. Esbensen, Nucl. Phys. **A352**, 147 (1981).

[6] H. Esbensen, Jian-qun Wu, and G. F. Bertsch, Nucl. Phys. **A411**, 275 (1983).

[7] N. Austern, *Direct Nuclear Reaction Theories* (Wiley, New York, 1970).

[8] W. J. Swiatecki, Phys. Scr. **24**, 113 (1981).

[9] G. Rangarajan, V. S. Ramamurthy, and S. K. Kataria, *Proceedings of the Symposium on Nuclear Physics and Solid State Physics* (DAE, Mysore, **26B**, 1983), Vol. 26B.

[10] V. Jahnke, H. H. Rossner, D. Hilscher, and E. Holub, Phys. Rev. Lett. **48**, 17 (1982).

[11] C. E. Aguiar, L. F. Canto, and R. Dunangelo, Phys. Rev. C **31**, 1969 (1985).

[12] M. Brack, J. Damgaard, A. S. Jensen, H. C. Pauli, V. M. Strutinskii, and C. M. Wong, Rev. Mod. Phys. **44**, 320 (1973).

[13] D. L. Hill and J. A. Wheeler, Phys. Rev. **89**, 1102 (1953).

[14] C. E. Aguair, V. C. Barbosa, L. F. Canto, and R. Donangelo, Phys. Lett. B **201**, 22 (1988).

[15] J. G. Keller, K. H. Schmidt, F. P. Hessberger, G. Munzenberg, W. Reisdorf, H. G. Clerc, and C. C. Sahm, Nucl. Phys. **A452**, 173 (1986).

[16] A. M. Stefanini, G. Fortuna, R. Pengo, W. Meczynski, G. Montagnoli, L. Corradi, A. Tivelli, S. Beghini, C. Signorini, S. Lunardi, M. Morando, and F. Soramal, Nucl. Phys. **A456**, 509 (1986).

[17] R. Pengo, D. Evers, K. E. G. Lobner, U. Quade, K. Rudolph, S. J. Skorka, and I. Weidl, Nucl. Phys. **A411**, 255 (1983).

[18] M. Beckerman, J. Ball, H. Enge, M. Salomaa, A. Sperduto, S. Gazes, A. DiRienzo, and J. D. Molitoris, Phys. Rev. C **23**, 1581 (1981).

[19] M. Beckerman, M. Salomaa, A. Sperduto, J. D. Molitoris, and A. DiRienzo, Phys. Rev. C **25**, 837 (1982).

[20] M. Beckerman, M. K. Salomaa, J. Wiggins, and R. Rohe, Phys. Rev. C **28**, 1963 (1983).

[21] W. Reisdorf *et al.*, Nucl. Phys. **A438**, 212 (1985).

[22] W. Reisdorf *et al.*, Nucl. Phys. **A444**, 154 (1985).